ISSN 1064-2269, Journal of Communications Technology and Electronics, 2019, Vol. 64, No. 10, pp. 1144–1148. © Pleiades Publishing, Inc., 2019.
Russian Text © The Author(s), 2019, published in Radiotekhnika i Elektronika, 2019, Vol. 64, No. 10, pp. 1029–1033.

Determination of the Parameters of Tunneling Barriers of Superconducting Tunnel Structures for Submillimeter Receivers

M. E. Paramonov[a], *, L. V. Filippenko[a], P. N. Dmitriev[a], M. Yu. Fominsky[a], and V. P. Koshelets[a]

[a] *Kotelnikov Institute of Radio Engineering and Electronics, Russian Academy of Sciences, Moscow, 125009 Russia*

**e-mail: paramonov@hitech.cplire.ru*

Received May 7, 2019; revised May 17, 2019; accepted May 21, 2019

Abstract—The parameters of the tunneling barrier of Nb/Al–AlO_x/Nb Josephson junctions were estimated in a wide range of current densities using the Simmons method. It is shown that with an increase in resistivity R_nS from 60 to 2100 Ω μm^2 (a reduction in the density of the tunneling current of junction J from 3.5 to 0.1 kA/cm^2), the height of the tunneling barrier increases from 0.85 to 1.18 eV and its width increases from 10.7 to 13.3 Å. The experimentally observed linear dependence of the tunneling barrier parameters on R_nS made it possible to estimate the capacitance of junctions in the range of R_nS 10–30 Ω μm^2 required to create low-noise submillimeter-range receivers.

DOI: 10.1134/S1064226919100115

INTRODUCTION

Research in the submillimeter wavelength range requires high-resolution spectrometric equipment operating at terahertz (THz) frequencies and having a very low intrinsic noise level. The most effective in this area are superconducting heterodyne receiving systems. One of the main elements of a heterodyne receiver is a mixer with a nonlinear current–voltage characteristic (CVC). The superconductor–insulator–superconductor (SIS) junction serves as a mixer in such a receiver [1–10]. The presence of a thin insulator layer in an SIS structure determines the presence of a significant capacitance that shunts the nonlinear resistance of the mixer at a high frequency. To achieve a mixer with low conversion losses and, as a result, reduce the mixer's self-noise to a level close to hf/k, the capacitance of the SIS junction must be compensated with additional inductance. Thus, to design high-quality and sensitive heterodyne receivers, it is necessary to know the exact capacitance value of the used SIS junctions.

To estimate the capacitance, one can use the measurement of the geometric and electric parameters of the tunnel junction. One of these parameters is the thickness of the insulation layer d. Since in the manufacture of an SIS mixer based on the three-layer Nb/Al–AlO_x/Nb structure, an AlO_x insulator layer is formed by the oxidation of Al, some of the metal remains unoxidized. Thus, the actual thickness of the AlO_x layer remains unknown. There is a universal method for determining the thickness of a tunneling barrier d, as well as its average height φ from the CVC at high voltages, by measuring the dependence of the tunneling current density on voltage. This dependence was proposed by Simmons [11] and generalized by Brinkman [12] for tunnel junctions in the low bias voltage limit.

The main characteristics of a metal–insulator–metal tunneling barrier are the average barrier height φ and its width d. These parameters can be used to judge the characteristics of the manufactured junctions, in particular, the properties of its thin insulating layer. In this case, it is assumed that a real asymmetric tunneling barrier can be approximated in a first approximation by a rectangle of width d and height φ (Fig. 1). As shown in [11], the current through the junction for an equivalent rectangular barrier is calculated by the formula

$$j = j_0\left(\varphi\exp\left(-B\sqrt{\bar{\varphi}}\right) - \left(\bar{\varphi} + eV\right)\exp\left(-B\sqrt{\bar{\varphi} + eV}\right)\right). \quad (1)$$

The following notation is used here:

$$j_0 = \frac{e}{2\pi h}\left(gd\right)^2, \quad B = \frac{4\pi d}{h\sqrt{2m}},$$

where $g \cong 1$ is the form factor, m is electron mass, V is constant voltage at the junction, and e is the electron charge. In the low bias voltage limit $eV \ll \varphi$, expression (1) is described with good accuracy by a parabolic dependence on the applied voltage V, which

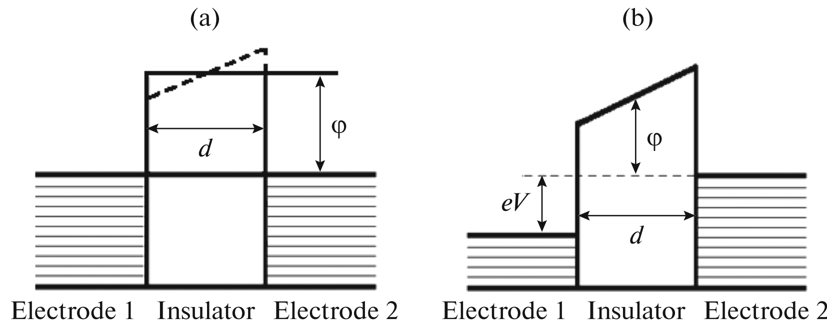

Fig. 1. Schematic diagram of potential barrier in SIS structures: (a) asymmetric barrier (dotted line) and rectangular barrier that approximates it (solid line) with $V = 0$; (b) case of intermediate bias voltages ($eV < \varphi$).

is usually represented as an expression for the differential conductivity G:

$$G = dI/dV = \alpha\left(1 + 3\gamma V^2\right), \tag{2}$$

where

$$\alpha = 3.16\times10^{10}\frac{\sqrt{\varphi}}{d}\exp\left(-1.025d\sqrt{\bar{\varphi}}\right), \tag{3}$$

$$\gamma = 0.0115\frac{d^2}{\bar{\varphi}} - 0.0315\frac{d}{\bar{\varphi}^{3/2}}, \tag{4}$$

In expressions (2)–(4), $\bar{\varphi}$ and V are measured in volts; G, in Ω^{-1} cm^{-2}; and the barrier thickness d in Å. The determination of the barrier parameters is also valid for niobium SIS junctions with a pronounced energy gap at a voltage of about 3 mV. Measurements are carried out in a relatively wide voltage range; therefore, the features associated with the junction energy gap are not taken into account and have no effect on further calculations. It can also be seen that measurements are carried out at low temperatures in order to eliminate the influence of series resistance of the supply electrodes and simultaneously monitor the quality of the formed tunnel junction.

The technology for manufacturing high-quality submicron tunnel junctions was developed and optimized at the Kotelnikov Institute of Radio Engineering and Electronics, Russian Academy of Sciences [8–10]; this technology has successfully been used to create integrated THz-band receivers [13–15]. Currently, receiving systems are being developed for new radio astronomy projects [15–17], including the receiving complex of the Millimetron space observatory [18], which operates in the 211–275 GHz range. Experimental samples of SIS mixers of this range were developed, manufactured, and investigated; Fig. 2 shows the CVC of the SIS mixer: an autonomous curve and the CVC under the action of radiation from a local heterodyne generator at a frequency of 265 GHz (the Josephson effect is suppressed by magnetic field). Junction resistance: $R_n = 38$ Ω, area $S =$ 0.73 μm^2, quality parameter $R_j/R_n = 27$, gap voltage $V_g = 2.85$ mV.

When measuring the parameters of the tunneling barrier, Nb/Al–AlO_x/Nb junctions were used. This type of junction is the most common and is used in most devices and circuits of low-temperature superconducting electronics. Resistivity R_nS for the studied junctions ranged from 20 to 2100 Ω μm^2.

Samples were made using thin-film technology on a high-resistance silicon substrate. All main layers of the junction were deposited on the substrate in a single vacuum cycle by magnetron sputtering. The AlO_x tunneling layer was created by oxidizing a thin Al layer at a constant oxygen pressure in the chamber. Then, photolithography and plasma-chemical etching were used to form the geometry of the junctions and supply electrodes. The finished sample contained up to 14 SIS junctions of various size. The measurements were carried out at liquid helium temperature. For each junction, the CVC ere measured in the voltage range of ±0.6 V.

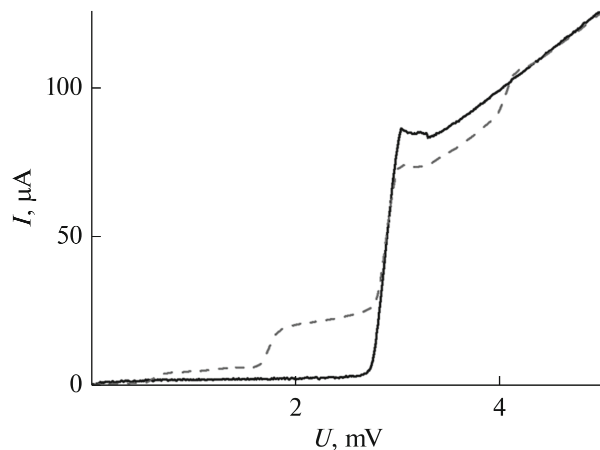

Fig. 2. CVC—autonomous (solid line) and under influence of heterodyne radiation at frequency of 265 GHz (dashed line)—of SIS mixer based on Nb/Al–AlO_x/Nb junctions; critical current suppressed by magnetic field.

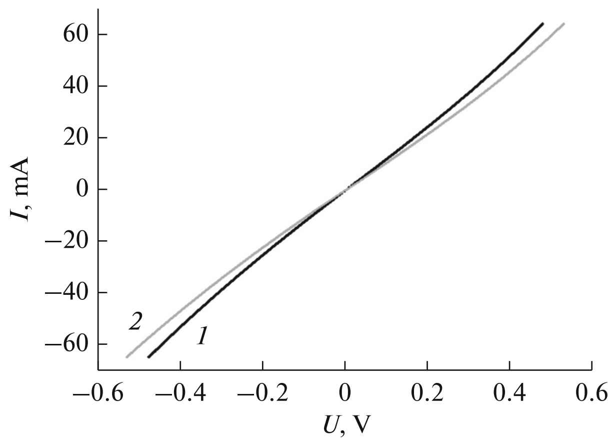

Fig. 3. CVC of tunnel SIS junctions prepared on same substrate and measured over large voltage range; curves with largest (*1*) and smallest (*2*) resistance are shown.

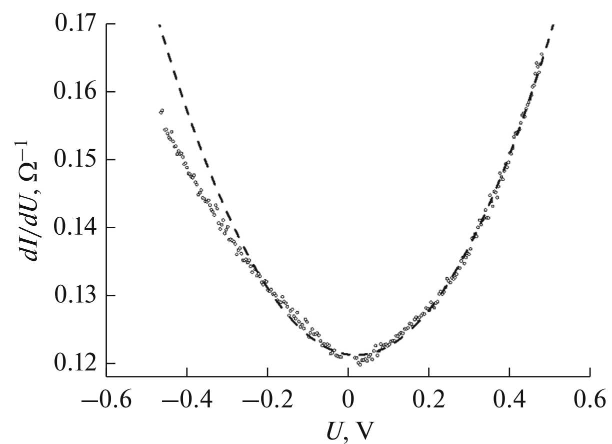

Fig. 4. Dependence of differential conductivity of tunnel SIS junction dI/dU on voltage (dots) and approximation by quadratic polynomial (dashed curve).

Figure 3 shows the CVC of the junctions made on one of the substrates. The characteristics are presented for two junctions: with the highest and lowest resistance; the remaining CVC lie between them. It is seen that as the voltage increases, the differential conductivity of the junction gradually begins to grow.

The voltage derivative (see Fig. 4) has a parabolic character and is approximated by a second-degree polynomial. Figure 4 shows that only the right branch falls quite accurately on the theoretical dependence. This is usually explained by the fact that this approximation, which is related to the representation of a rectangular barrier, is far from the real situation; similar results were observed in [19], which investigated Nb/Al–AlO_x/Nb junctions. Measurements in a wider voltage range (up to 1 V) and subsequent approximation showed the presence of a region with a stronger change in the differential conductivity on one branch of the curve. That is, the theoretical curve as a whole coincides with the experimental dependence, except for a certain area of the left branch, which in our case looks like a "misaligned" dependence.

Table 1. Measured and calculated data for different SIS junctions

Sample name	Measurements	Calculation	
	R_nS, Ω μm²	φ, V	*d*, Å
U06#1	61	0.85	10.71
SQ#1	141	0.88	11.49
SQ#4	247	1.03	11.52
LT07	1300	1.19	13.21
U05	1377	1.14	12.86
U03_05#01	1453	1.17	12.78
U12#2	1663	1.1	13.64
U12_2#2	2025	1.18	13.27
U12_2#1	2112	1.18	13.3

To calculate the parameters of the barrier of this junction, a theoretical curve is used only for the right branch. From its equation, it is possible to obtain values of α and γ, where α, in fact, is the value of the junction conductivity at zero bias voltage—the minimum of the parabola; parameter γ is in turn proportional to the ratio of the coefficient for the term in the polynomial equation quadratic to α. The values of the height and width of the tunneling barrier φ and *d* are obtained by solving the system of equations by numerical methods. In [19, 20], the estimates of the height and width of the tunnel barrier by J. Simmons' formula are compared with the results of a more accurate calculation; the effect of the difference in effective masses in the metal and barrier is also investigated. It is estimated that the effective electron mass in the barrier is equal to half the electron mass in the metal; therefore, in our calculations, we used the additional parameter $m_{eff} = 0.5m_0$. Table 1 presents the data with the measurement and calculation results. For each sample, the parameters ϕ and *d* were calculated taking into account the effective mass. For junctions with a sufficiently large R_nS (about 100 Ω μm²), it was not particularly difficult to determine the tunneling barrier parameters: the curves were easily approximated by a parabola along one of the branches, but difficulties arose for junctions with a small R_nS. As an example, Fig. 5 shows the dependence of conductivity on voltage for sample U06#1 with R_nS = 61 Ω μm². In general, the curve has a parabolic character, but the graph clearly shows areas of a sharp drop in the junction conductivity at the same voltage values above and below zero. These features are not related to overheating and breakdown of the sample or the influence of the measuring electronics. Experiments to check the distortion related to overheating were carried out using

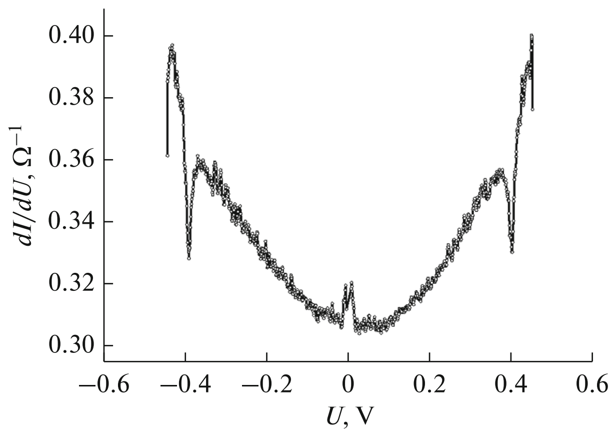

Fig. 5. Dependence of differential conductivity of tunnel SIS junction dI/dU on voltage with features at voltages of ±400 mV.

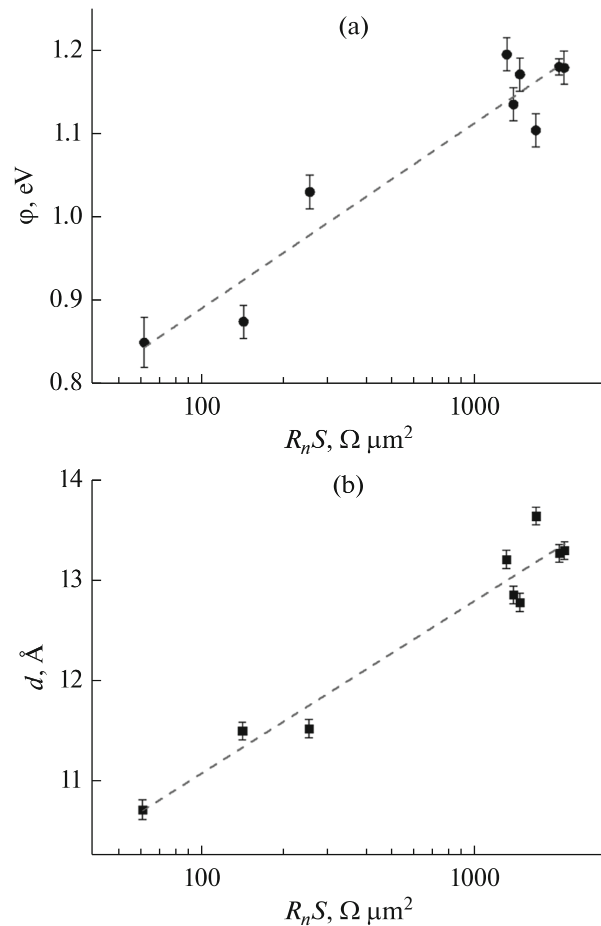

Fig. 6. Dependence of height (a) and width (b) of tunneling barrier on R_nS: points, experiment; dashed curves, linear approximation.

a pulsed voltage source with a variable duty cycle of the applied signal. Distortions in the shape of the parabolic dependence become more appreciable for samples with an even smaller R_nS (<50 Ω μm^2). A possible cause of these effects may be electron–phonon interaction; additional experiments are planned to determine the nature of these phenomena. Thus, we can conclude that the method described above for determining the parameters of tunneling barriers has some limitations for samples with a low R_nS.

Based on the data obtained as a result of the calculations, the dependences of the height and width of the tunneling barrier on R_nS were constructed (Fig. 6). The vertical lines in the figures indicate the ranges of errors associated with inaccuracies in approximating the dependences of the differential conductivity of the junction on the applied voltage $G(V)$ of an ideal parabola, and the entire series of samples was linearly approximated, showing a characteristic increase in the height and width of the barrier with increasing R_nS. Figure 6 shows that the plots of the height and width of the barrier on R_nS have a clear linear character on a semilogarithmic scale and make it possible to estimate the capacitance of tunnel structures, which is necessary for designing submillimeter range receiving systems. It should be noted that the parameter of the effective electron mass strongly influences the final calculation results. Without this correction, the barrier height would be 0.2 eV greater than the given one, and the barrier width would be 3.7 Å smaller.

It is known that to obtain a sufficiently wide matching band of the mixing element, junctions with a very high current density are required. Difficulties encountered in determining the parameters of barriers with high tunneling current density (resistivity less than 100 Ω μm^2) associated with the features of CVC did not allow estimation of the parameters in the region most important for THz mixers [17, 18]. However, the linearity of the graphs at the chosen scale allows extrapolation of the dependences to the region of small R_nS values. The values of the real thickness of the tunneling barrier defined in this way were used to estimate the junction capacitances when designing receivers.

Estimation of the tunnel junction capacitance, based on the real values of the thickness of the tunneling layer, made it possible to develop more advanced and properly matched receiving systems. For example, for an SIS junction area of 0.73 μm^2 and R_nS = 27.9 Ω μm^2 acting as a mixer in the integrated receiver in the 211–275 GHz frequency range with a center frequency of 240 GHz, the value of the calculated specific capacitance was 88 fF/μm^2. To achieve a low noise temperature of the receiver, it was necessary to compensate the capacitance of the SIS junction in the operating frequency range and match the impedance of the SIS junction at high frequency (about 30 Ω) with a waveguide impedance of about 400 Ω. This was achieved by incorporating an SIS junction into a planar structure consisting of segments of coplanar and microstrip

$Nb/SiO_2/Nb$ lines. Such a design made it possible to compensate the junction capacitance at the operating frequency and to match the resulting low impedance with the waveguide. The noise temperature of the receiver (measured in double side band mode, DSB) was 25 K at a frequency of 265 GHz [21], which is only twice the quantum sensitivity limit hf/k_B.

CONCLUSIONS

The $Nb/Al–AlO_x/Nb$ tunnel junction characteristics were measured; these are widely used in most devices and circuits of low-temperature superconducting electronics, including for creating ultrasensitive submillimeter-range receivers, The dependence of the height and width of the tunneling barrier on the density of the tunneling current (resistivity of junctions) was found; it was shown that the linear nature of the dependences makes it possible determine the capacitance of tunnel structures with a specific resistance of 10–30 $\Omega\ \mu m^2$, for which direct measurements become impossible. Correct estimation of the capacitance of SIS mixers made it possible already in the first experiments to obtain a noise temperature of 25 K at a frequency of 265 GHz, which is only twice as large as hf/k_B.

FUNDING

The study was financed by the Russian Science Foundation (project no. 19-19-00618); USU 352529 was used for fabrication of the SIS junctions. The tunnel structures were manufactured at IREE RAS in the framework of the state task.

REFERENCES

1. J. M. Rowell, M. Gurvitch, and J. Geerk, Phys. Rev. B **24**, 2278 (1981).
2. H. A. Huggins and M. Gurvitch, J. Appl. Rhys. **57**, 2103 (1985).
3. M. Gurvitch, M. A. Washington, and H. A. Huggins, Appl. Phys. Lett. **42**, 472 (1983).
4. S. I. Morohashi, F. Shinoki, A. Shoji, et al., Appl. Phys. Lett. **46**,1179 (1985).
5. T. Imamura and S. Hasuo, IEEE Trans. Appl. Supercond. **2**, 84 (1992).
6. J. R. Tucker, IEEE J. Quantum Electron. **15**, 1234 (1979).
7. J. R. Tucker and M. J. Feldman, Rev. Mod. Phys. **57**, 1055 (1985).
8. V. P. Koshelets, S. A. Kovtonyuk, I. L. Serpuchenko, et al., IEEE Trans. Magn. **27**, 3141 (1991).
9. L. V. Filippenko, S. V. Shitov, P. N. Dmitriev, et al., IEEE Trans. Appl. Supercond. **11** (1), 816 (2001).
10. P. N. Dmitriev, I. L. Lapitskaya, L. V. Filippenko, et al., IEEE Trans. Appl. Supercond. **13**, 107 (2003).
11. J. G. Simmons, J. Appl. Rhys. **34**, 1793 (1963).
12. W. F. Brinkman, R. C. Dynes, and J. M. Rowell, J. Appl. Phys. **41**, 1915 (1970).
13. V. P. Koshelets, S. V. Shitov, A. B. Ermakov, et al., IEEE Trans. Appl. Supercond. **15**, 960 (2005).
14. V. P. Koshelets, A. B. Ermakov, L. V. Filippenko, et al., IEEE Trans. Appl. Supercond. **17**, 336 (2007).
15. V. P. Koshelets, P. N. Dmitriev, M. I. Faley, et al., IEEE Trans. Terahertz Sci. Technol., **5**, 687 (2015).
16. A. Khudchenko, A. M. Baryshev, K. I. Rudakov, et al., IEEE Trans. Terahertz Sci. Technol. **6**, 127 (2016).
17. K. I. Rudakov, V. P. Koshelets, A. M. Baryshev, et al., Radiophys. Quant. Electron. **59**, 711 (2017).
18. A. V. Smirnov, A. M. Baryshev, P. de Bernardis, et al., Radiophys. Quant. Electron. **54**, 557 (2012).
19. S. K. Tolpygo, E. Cimpoiasu, X. Liu, et al., IEEE Trans. Appl. Supercond. **13** (2), 99 (2003).
20. L. P. Bulat, V. V. Konopel'ko, and D. A. Pshenai-Severin, Vestn. Mezhdunar. Akad. Kholoda, No. 3, 46 (2013).
21. K. I. Rudakov, A. M. Baryshev, R. Hesper, et al., in *Program and Abstract Book, 30th Int. Symp. on Space Terahertz Tech., Gothenburg, Apr. 15–17, 2019* (Chalmers Univ. Tech., Gothenburg, 2019), p. 61.